Applications of the Sediment-Transport Path Model to the Tidal Flats of Garolim Bay, West Coast of Korea

Dong-Hyeok Shin,* Hi-Il Yi*, Sang-Joon Han*, Jae-Kyung Oh+, and Joong-Sun Won*

*Marine Geology and Geophysics Division, Korea Ocean Research and Development Institute, Ansan P. O. Box 29, Seoul 425-600, Korea (Tel : 0345-400-6263, hilee@sari.kordi.re.kr)

+Department of Oceanography, Inha University, Incheon 402-651, Korea

(manuscript received 12 December 1995)

Abstract

Bidirectional transport trend using the sediment-transport path model was identified in the two areas, sand ridge area and tidal mudflat in Garolim Bay, which is located in the mid-western coast of Korean Peninsula. This model exhibits the two-dimensional view of clear sediment transport trend based on data of changes in sediment statistics such as mean, sorting, and skewness. Garolim Bay was selected to test for the sediment-transport path model developed by *McLaren and Bowles* [1985]. Line-S, a typical tidal mudflat and representative of the Garolim Bay tidal flats, is well tested by this model, showing a clear seasonal change and coarsening-trend seaward (case C). This indicates that strong ebb currents carried relatively coarser sediments seaward with respect to high energy regime. Seasonally, this energy regime slowly decreases toward the summer in contrast with an increase of energy regime of flood tides, carrying coarser sediments landward (case C) in the summer. However, the Line-D area does not show consistent transport trend with respect to time-series. Separated and scattered events show fining trend landward (case B) in the sand ridge itself. The finining-trend (csae B) either seaward and landward is not chiefly important in both the entire Line-D area and the sand ridge itself. Also, the coarsening-trend (case C) landward is not sighificant in the sand ridge itself. Consequently, in reality, the selection of suitable and representative locations are very important to fit with this model.

1. Introduction

Garolim Bay is located in the Taean Peninsula, the mid-western coast of Korea (Figs. 1 and 2). This bay was studied by coastal engineers in order to survey a feasibility of tidal power plant [*Korea Ocean Research and Development Institute*, 1981, 1993; *Song et al.*, 1983].

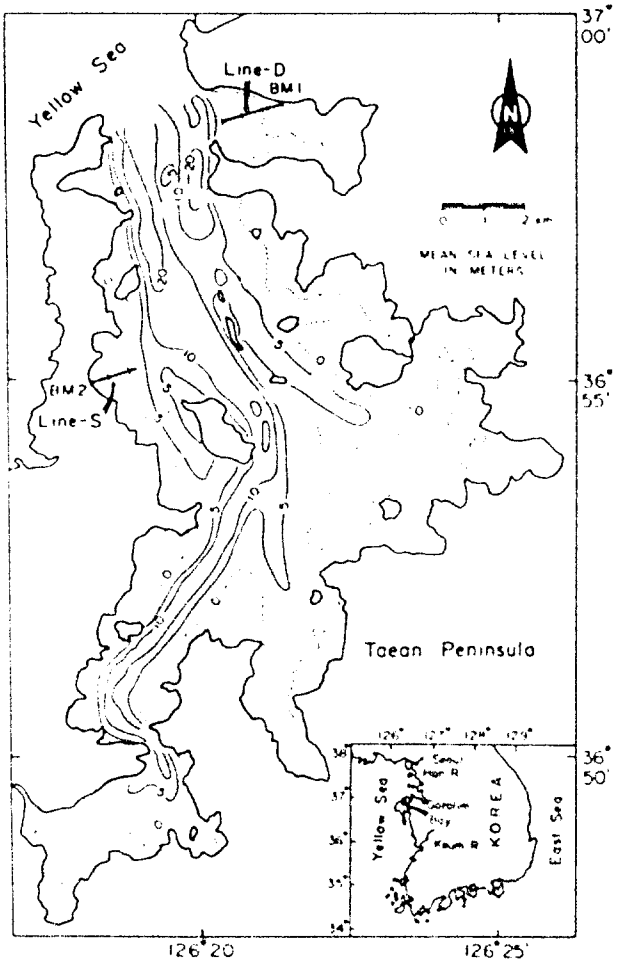

Fig. 1. The bathymetry map of Garolim Bay, showing Line-D in the northeastern corner and Line-S in the western part of the bay.

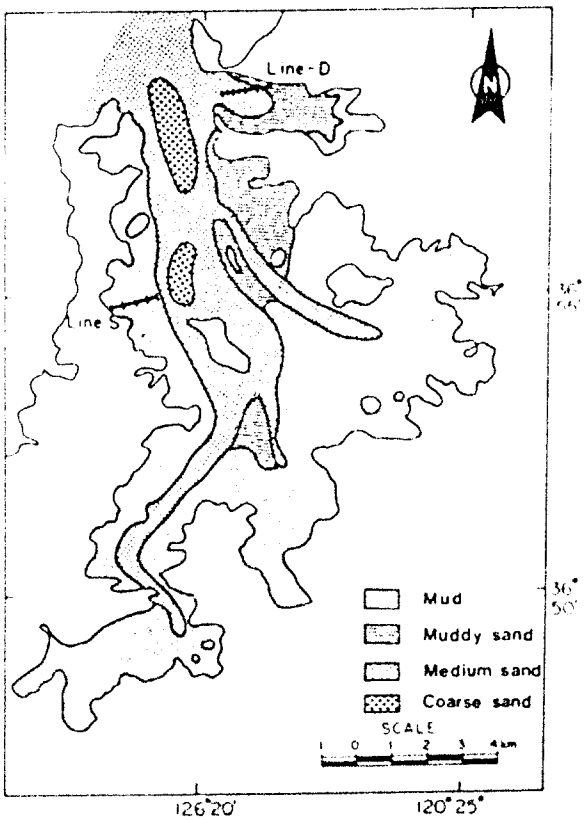

Fig. 2. The surface sediment distribution of Garolim Bay, showing Line-D in the sand ridge and muddy sand area, and Line-S in the pure mud area.

In this bay, sedimentological studies were not conducted previously except for clay mineralogical work [*Han*, 1982] and general surface sediment pattern in the bay [*Song, et al.*, 1983]. Recently, sedimentological work such as understanding of sediment processes [*Shin, et al.* 1995a, 1995b; *Shin et al., in press* (1995c); *Yi et al.*, 1995], and stratigraphy [*Yi, et al., in press* (1996)] was attempted. However, the mathematical determination of sediment processes was never conducted on the surface

of coastal areas in the Korean Peninsula. In this paper, the quantitative trend of sediment transport was first conducted using the sediment-transport path model developed by *McLaren and Bowles* (1985). The sediment-transport path model is well applicable in a flume experiment (*Day*, 1980) and distinct unidirectional environments in reality (*Emmett et al.*, 1980; *Pickrill and Irwin*, 1983; *McLaren and Bowles*, 1985). In the study area, two distinctive transport directions are presented due to the tides. Bidirectional environments are also first empirically tested using this model. Therefore, it might be more complicated situations for sediment-transport and need to be considered more implicit geological interpretations of sedimentary environments. The factors to fit into the best conditions for the sediment-transport path model are : 1) sediments are transporting unidirectionally; 2) the source of sediments should be one origin; 3) transported sediments are compared among concurrent events. Garolim Bay is a suitable environment for satisfying the above three conditions except for the first condition because the tides cause the bidirectional trend. However, there has been no survey of bidirectional transport environments statistically tested by the sediment-transport path model. It is important to apply this model to tidal flat environments. Therefore, we can be able to compare transport directions during sequential events as well as one event because five periodical monitorings were conducted from Oct. 1994 to June 1995 (8 months).

2. Sediment-Transport Path Model

Sediment transport mechanisms, resulting in either erosion or deposition, affect grain-size frequency distributions such as the mean, sorting, and skewness. The initial concept of sediment transport model is as follows. First, when we choose any grain-size distribution, $g(s)$ (Fig. 3), the transported grain-size distribution ($r(s)$) which is derived from $g(s)$ according to a function $t(s)$ is expressed as :

$$r(s_i) = kg(s_i) = kg(s_i)\, t(s_i)$$

or

$$t(S_i) = \frac{r(S_i)}{kg(S_i)}, \qquad (1)$$

where $k(S_i)$ and $r(S_i)$ define the proportion of the sediment in the ith grain-size class interval for each of the sediment distributions. k is a scaling factor that normalizes $r(s)$ so that

$$\sum_{i=1}^{N} r(s_i) = 1$$

Thus,

$$k = \frac{1}{\sum_{i=1}^{N} g(s_i)\, t(s_i)}$$

The remaining sediment, $d(s)$, has new distribution after the removal of $r(s)$ from $g(s)$ (Fig. 3), where

$$d(s_i) = \mathrm{k}' g(s_i)\,(1 - t(s_i))$$

or

$$t'(s_i) = \frac{d(s_i)}{k' g(s_i)}$$

where

$$t'(s_i) = 1 - t(s_i)$$

and

$$k' = \frac{1}{\sum_{i=1}^{N} g(s_i)\,(1 - t(s_i))}$$

Here, $t(s)$ is statistically described as all of the processes which move sediment from one location to another as well as used distribution functions for sediment size. The function of $t(s)$ is presenting a size distribution function (such as weight proportion, grain-size frequency, etc).

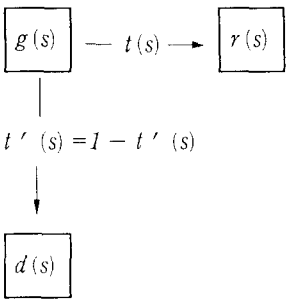

Figure 3. Schematic diagram of the basic sediment-transport model. This diagram was fully discussed in the text.

Therefore, each $t(s_i)$ provides the probability of conveying grains of size "s_i" from a grain-size distribution of source ($g(s)$) to a new distribution by transportation ($r(s)$). *McLaren and Bowles* [1985] proposed to call each $t(s_i)$ a transfer coefficient and $t(s)$ a sediment-transfer function. The simple concept of $t(s)$ was proven to be effective for deciding sediment-transport paths and each interrelationships among sediment transportation and new distributions on the basis of a decreasing or increasing functions (on a phi(ϕ) scale) linearly and monotonously [*McLaren et al.*, 1981; *McLaren*, 1984]. The assumption in which $t(s)$ is monotonously increasing indicates that sediment by transportation ($r(s)$) is always finer and more negatively skewed than its source ($g(s)$) and that the lag ($d(s)$) is always coarser and more positively skewed than its source ($g(s)$). Sorting must ultimately become better in both the sediment in transport and in the lag.

McLaren and Bowles [1985] applied the above simple sediment-transport model to broad sediment distributions in practice. When we choose several stations linearly along the direction of transport, remaining grain-size distributions can be $d_1(s)$, $d_2(s)$, $d_3(s)$, . . . , respectively. Transported sediments are expressed by $r_1(s)$, $r_2(s)$, $r_3(s)$, ... When we consider the first sediment transport function ($t_0(s)$) is equal to 1 for all "s", $r_1(s) = g(s)$. This distribution ($r_1(s)$) is resulted from the function $t_1(s)$ which produces a new distribution by transportation $r_2(s)$ and the remaining sediment $d_1(s)$. The denotation $d_1(s)$ has a relationship with $r_1(s)$ by the function 1 - $t_1(s)$. Nearly, $r_2(s)$ is acted upon by $t_2(s)$ resulting in another new distribution $d_2(s)$.

Expanded sediment-transport model in Figure 4 contains basic three boxes in any single event in Figure 3 using the assumption of monotonous increase of $t(s)$.

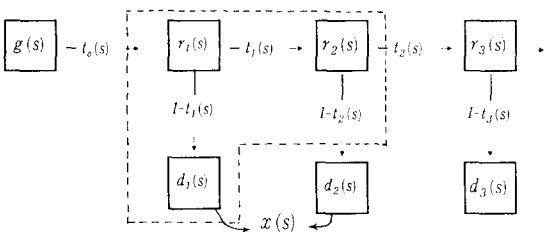

Fig. 4. Schematic diagram of the expanded sediment-transport path model. The three boxes enclosed by the dotted-line are analogous to the basic sediment-transport model shown in Figure 3. The definition of terms is explained in the text.

Consequently, the sequence of transported sediments ($r_1(s)$, $r_2(s)$, $r_3(s)$, . . ., *etc.*) must be changed progressively to finer and more negatively skewed (more excess of finer grained). On the other hand, each $d(s)$, remaining lag sediments become coarser and more positively skewed (more excess of coarser grained). For instance, $d_3(s)$ is coarser and more positively skewed than $r_3(s)$ (Fig. 4).

Since $r(s)$, $t(s)$, and (occasionally) $g(s)$ are not able to be observable, the relative changes in sediment distributions among the sequential lags, $d_1(s)$, $d_2(s)$, $d_3(s)$, . . can be determined. Therefore, we can consider that $d_2(s)$ is related to $d_1(s)$ by a function $X(s)$, so that

$$d_2(s) = k d_1(s) X(s)$$

where

$$k = \frac{1}{\sum_{i=1}^{N} d_i(s_i) X(s_i)}$$

or

$$X(s) = \frac{d_2(s)}{kd_1(s)}$$

As shown in Figure 4, $d_2(s)$ can also be related to $d_1(s)$ by

$$d_2(s) = \frac{kd_1(s)\,t_1(s)\,(1-t_2(s))}{1-t_1(s)}$$
$$= kd_1(s)\,X(s)\,kd_1(s)\,X(s)$$

where

$$X(s) = \frac{t_1(s)\,(1-t_2(s))}{1-t_1(s)} \qquad (2)$$

$X(s)$ is a combined function of two transfer functions $t_1(s)$ and $t_2(s)$. Also, $X(s)$ can be considered a transfer function by the statistical relationship between two sequential deposits. Alike to $t(s)$, $X(s)$ incorporates all of the processes, forming sediment transport and redistribution during a certain period represented by the samples. As result, the relative change in the distributions from $d_1(s)$ to $d_2(s)$ relies upon the shape of function $X(s)$ which can be determined by the empirical examination of $t(s)$ functions.

Now, we can apply the above model to natural environments for which the sediment-transport directions are known. From the models presented in Figures 3 and 4, grain-size distributions become changing to either more erosional or more depositional patterns in which remaining sediments $(d(s))$ must be coarser and more positively skewed than their sources (case A), while sequential deposits can become either finer and more negatively skewed (case B) or coarser and more positively skewed (case C). As mentioned before, sorting or variance must eventually become better in each of three cases. If case A and case C have the same trends, it indicates that there is no transportation in direction. However, if there are difference in trends between case A and case C, this will provide the important geological changes in that environment.

3. Methods and Applications

Natural environments are not as simple as the laboratory settings such as flume experiments due to many complicated factors involved in the original source $(g(s))$. In this paper, a statistical method was applied to determine the transport direction of source sediment $(g(s))$ and its sequential deposits $(d(s))$ by examining all possible pairs in a sample suite [*McLaren and Bowles*, 1985]. When we select n samples, there are $n^2-n/2$ directionally oriented pairs that may present a trend suggesting transport in one direction, and an equal number of pairs in the opposite direction. Compared between any two samples with respect to mean size, sorting, and skewness, eight possible trends exist. They are: 1) finer (F), better sorted (B), and more negatively skewed (-); 2) coarser (C), more poorly sorted (P) and more positively skewed (+); 3) C, B, -; 4) F, P, -; 5) C, P, -; 6) F, B, +; 7) C, B, +; or 8) F, P, +. Among eight trends above, only two can provide a transport direction, i.e., F, B, - (case B), and C, B, + (case C), presenting a one-eighth probability of either occurring at random ($p = 0.125$). Due to the uncertainty related to variance (sorting), the cases of better sorting are chosen for the two cases indicating transport direction. Two hypotheses are tested in the case of the number of occurrences of a particular case exceeding the random probability of 0.125.

H_0 : $p \leq 0.125$, suggesting no preferred transport direction, and

H_1 : $p > 0.125$, suggesting a preferred transport direction.

the Z-score [*Spiegel*, 1961] is used in a one-tailed test, so that H_1 is accepted if

$Z = x - Np / \sqrt{Npq}$ > 1.645 (0.05 level of significance)

or

> 2.33 (0.01 level of significance),

where x = observed number of pairs representing a particular case in one of the two opposing directions; and N = total number of possible unidirectional pairs. $N = n^2 - n/2$ where n = number of samples in the sequence; p = 0.125; and q = 1.0 - p = 0.875.

The Z-statistic is considered valid for N > 30 (i.e., a large number). Therefore, in this case, a suite of 8 or 9 samples are the minimum required to evaluate validity in a transport direction (i.e., $9^2 - 9/2 = 36$, the total possible pairs in one direction)

4. General Setting of Study Area : Garolim Bay

The size of Garolim Bay is about 18 km in length and about 8 km in width with a narrow baymouth of only less than 3 km, resembling of a gourd-shape (Figs. 1 and 2). There is no major sediment input from the land due to no major river systems, except in a rainfall season [*Song et al.*, 1983]. Two main channels with a maximum of 25m in water depth exist at the baymouth, producing the sandbank deposits in the center (Fig. 2). In these two distinctive channels, flood currents are dominated in the west channel, while ebb currents are dominated in the east channel, creating a clockwise circulation. These channels are further divided into several tributaries toward the inner bay. In the middle of bay, the current circulations is conversely anticlockwise.

The tides in the bay are semi-diurnal with significant diurnal inequality and mean tidal range of about 4.63*m* (mean spring tidal range of 6.39 m; mean neap tidal range of 2.86*m*) [*Korea Ocean Research and Development Institute*, 1981; *Song et al.*, 1983]. The prevailing wind direction is northwest with the speed of higher than 13.0 m/sec during the winter [*Korea Ocean Research and Development Institute*, 1981; *Korea Meteorological Administration*, 1991]. Most of waves are locally wind-generated rather than swell propagated from offshore. Significant waves of larger than 1.5 m occur from October to March but about three fourth of the year are fair weathers [*Korea Ocean Research and Development Institute*, 1981]. The frequency of storms with wind speeds over 13.0 m/sec in the winter is 4 times greater than that in summer [*Korea Meteorological Administration*, 1989].

Annual mean precipitation is 1,234.9mm [*Korea Meteorological Administration*, 1981], exclusively falling during the summer of July to August. Water temperature widely varies from 0.8℃ in the winter (January and February) to 22℃ in the summer (August). The water temperature difference between surface and bottom layers is approximately 0.6-4.0℃ in the summer and 0.6-2.6℃ in the winter [*Korea Ocean Research and Development Institute*, 1981]. Salinity ranges from 30.6‰ in the summer to 32‰ in the winter. A decreasing trend of salinity in the summer is due to higher temperature and more rainfalls.

The geology surrounding Garolim Bay is composed of cliffed Precambrian schists and gneisses, Jurassic granites in the hillsides and mountains (about 100-300 m high), and Quaternary deposits in the coastal plains. Unlike other bays in the western coast of Korea, Garolim Bay is still immune from the major construction of seawalls and power plant. Nowadays, the ongoing survey for the feasibility of tidal power plant in Garolim Bay is conducted by coastal engineers [*Korea Ocean Research and Development Institute*, 1993]. Therefore, it is crucial to study sedimentary processes and environments in the condition of natural setting before artificial construction could modify or completely change this area. Realistically, it is difficult to find natural sedimentary environments of the bays and

tidal flats along the western coast of Korea.

The distribution of surface sediments in the bay consists mainly of sands in the baymouth and the main tidal channels, whilst tidal flats in the inner bay comprises mostly muds (Fig. 2). Coarse sands are formed in the sandbank of the baymouth and the western channel in the middle of bay. Gravels are dominant in some tidal channels, the rocky cliffs, and some beaches.

5. Study Locations : Line-D and Line-S

The two contrastive localities, Line-D and Line-S, are chosen for the comparison of changes in surface sediment patterns (Figs. 1 and 2). Both Line-D and Line-S were punctiliously measured at each 100*m* in distance, installed by iron stakes for the station positions. Line-D, 1,550*m* in a whole distance contains 16 stations (stations D1 to D16) from the bench mark to the edge of the main tidal channel during the ebb time of spring tide. At the edge of the main tidal channel (near mean low water level of subtidal zone), the distance from stations D15 to D16 is only 50 m. In the case of Line-S, 14 stations (stations S1 to S14) were marked with iron stakes with a 100 m interval except from stations S12 to S14 (50 m interval from stations S12 to S13 and only 30m interval from stations S13 to S14). Therefore, the total distance of Line-S is 1,280 m. The number of stations in both areas is increased seaward.
Occasionally, stations D16 in Line-D and S14 in Line-S were not completely exposed if it is not a spring tide, so that the collection of surface sediments and measurement of sedimentation rates were not able to be conducted in this case.

The elevation of surface morphology at each station of both Line-D and Line-S was meticulously measured twice (Oct. and Dec. 1994) using a leveler and a tape measure. Acrylic base-plates (30 x 30cm^2), firmly holded by two iron bars, were buried under the surface of about 30-50cm deep for measuring sedimentation rates. For each two month interval during Oct. 1994 - June 1995, sedimentation rates were measured by a vernier caliper at each station.
Simultaneously, surface sediments were cautiously collected right on the very surface for examining changes of grain-sizes in each two-month period. Field observations including characteristics of sedimentary structures and morphology were all recorded in detail with photographs. Surface sediment samples were wet-sieved to separate the sand and mud fractions after eliminating carbonate and organic matters, using by solutions of 0.1N HCl and 10% H_2O_2, respectively. The sand fractions (coarser than 4(ϕ), 0.0625 mm)) were sieved with a 0.5ϕ in size intervals [*Folk*, 1974]. The mud fractions (finer than 4ϕ) were mixed with a solution of sodium metaphosphate and put in an ultrasonic bath to disaggregate flocculated particles. Then they were analyzed using a SediGraph 5000D. Sediment statistics were calculated using the moment methods [*Griffith*, 1967].

6. Surface Morphology

The elevation pattern of the surface on both Line-D and Line-S is shown in Figure 5. In the two-dimensional view, Line-S has a simple elevation, gently decreasing seaward with slope angles of 0.08 from the land to station S11, but the slope angles from stations S11 to S14 is about 1.31, which are 16 times greater. On the other hand, the elevation of Line-D does not show a simply seaward decreasing trend. From the bench mark, it crosses the tidal channel before reaching the lee side of sand ridge. This tidal channel, approximately 1.5 km long and 300 m wide, is parallel to the northside of the land and the crest of sand ridge at each side. The seaside of this channel is merging to the eastern side of main channel

at the baymouth. The seaside of Line-D meets the east tidal channel near the baymouth, while that of Line-S reaches the west tidal channel in the middle of the bay (Fig. 2).

6.1. Line-D

Surface sedimentary distribution as well as morphology of Line-D is shown in Figure 5.

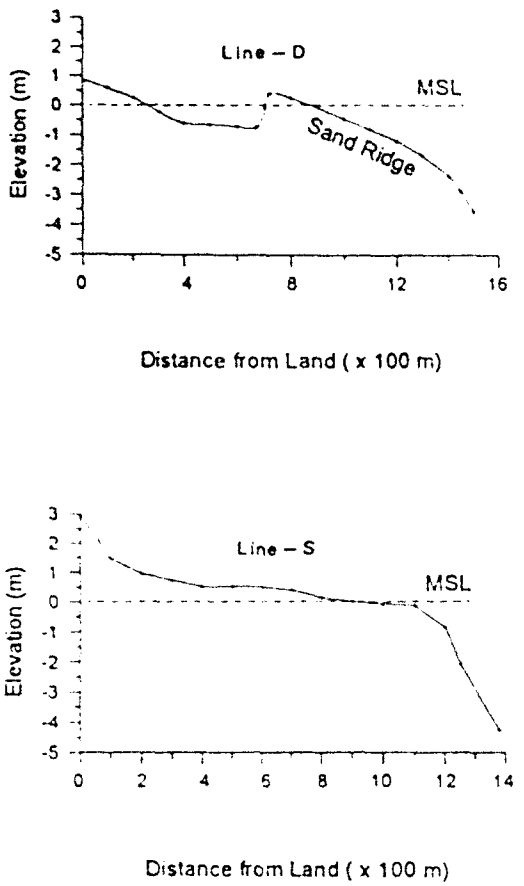

Figure 5. The shape of elevation of Line-D and Line -S. Line S contains much simpler trend from the land to the sea. On the contrary, the area of Line-D comprises more complicated geomorphic features than the area of Line-S.

Along the northside of the land, well-rounded gravel beaches exist. These gravels, mostly consisting of Precambrian gneisses and schists, are originated from outcrops of local area. Mostly silty sands are deposited from the land to about 300 m seaward. This silty sand area contacts smoothly adjacent to the tidal channel (about 300 m wide). These sediments are believed to be chiefly transported in suspension through the channel. No sedimentary structures are developed except a juvenile stage of parallel ripples appeared very briefly and disappeared again. Rocks, about 20 cm in average diameter and believed to be a result of natural and artificial ones, are scattered in this channel. Elongate mud mounds tapering off mostly landward during the ebb are blocked by these large scattered rocks. Parallel ripples are often developed on the mud mounds. During the time of ebbs and floods, the position and shape of these structures are rapidly moving and changing. Oysters, *Crassostrea giggas*, are attached on these rocks, providing a good natural oyster farm in this channel. The southern side of this channel is abruptly ended by the lee side of sand ridge, about 700 m in distance from the bench mark. Parallel to linguoid ripples with spreaded shell fragments, mostly oyster shell fragments, in the lower slope of the lee side are presented but large ripples such as lunate ripples are developed on the upper slope of the lee side. These lunate ripples are extended to the crest and the uppermost part of stoss-side. The crest of this sand ridge is about 2 m in height from the bottom of the channel, and the position, morphological pattern, and height were slightly changed, mostly landward during the repeated survey times. Small parallel ripples within and normal to lunate ripples are well developed on the crest of sand ridge. The stoss-side of sand ridge is about 800 m wide, eventually reaching the edge of main tidal channel, also called the subtidal zone. Small parallel, linguoid, and wave ripples are presented on the sand ridge. A thin belt

(about 10-30 m wide and 600 m long) of oyster field is located in the middle of sand ridge (between stations D9 and D10; see Fig. 5) parallel to the crest of sand ridge. Also, very shallow creeks, less than a few cm, meander on the sand ridge. Among these tidal creeks, two flow each side of the thin oyster belt.

6.2. Line-S

In Line-S, surface morphology is very monotonous except for meandering tidal creeks (a few cm to over 50 cm deep) (Fig. 5). Some tidal creeks, especially on the middle of Line-S, are very stabilized, so that the rounded shape of tidal surface is developed by these creeks. Most of surface are intensively bioturbated by crabs. Near the bench mark, water-saturated muds are mixed with some granules on the surface. These granules are come from the soils of the land. Some of the landside are, at present, built by about 1 to 2 m walls to protect the agriculture fields from the erosion of soils. oxidized coarse sands with a slightly mixture of dark gray tidal mud are presented at the sharp boundary of the walls, directly contacting the tidal zone. These oxidized coarse sands are originated from the soils of local area. Patched distributions of medium-to-fine sands, believed to be eolian or storm deposits, are piled at the boundary of the walls or irregular rocky places, occasionally covered the oxidized coarse sands. Salt marsh plants, *Salicornia sp.*, are sporadically growing at the edge of landward side of tidal flats (from the bench mark to stations S1 to S2). These wet mudflats are continuously extending about 300 m seaward. Some intensive burrows, mostly crab holes, are found in these areas. From stations S4 to S7, the surface morphology is slightly higher than adjacent stations on Line-S. Consequently, the surface is relatively harder than surrounding areas. Oyster shell fragments were scattered on the mud surface of stations S7 to S10. Suddenly, the surface of stations S11 to S14 is very wet, and it is even very hard for people to walk. Wood branches, attached by oysters, are spreaded at station S12 and surrounding areas (about 30 m wide). Both stations 13 and 14 are located near the subtidal zone.

7. Applications of Sediment-Transport Path Model to Garolim Bay

7.1. Line-D

The whole Line-D area, including inward muddy sand flat and oyster field is tested first. But sand ridge itself is also tested separately in order to observe a behavior of sand movement. Table 1 shows the number of pairs of the whole Line-D and sand ridge producing transport trends.

Table 1. The numbers of pairs of the whole and sand ridge itself of Line-D in Garolim Bay producing transport trends. N, x, and Z are defined in the text.

		Line-D (whole)				Line-D (Sand Ridge)			
Period		Seaward		Landward		Seaward		Landward	
		B	C	B	C	B	C	B	C
Nov. 94	N	120	120	120	120	36	36	36	36
	x	4	17	19	14	0	3	19	6
	Z	-3.0	0.6	1.1	-0.3	-2.3	-0.6	7.3	0.8
Dec. 94	N	136	136	136	136	45	45	45	45
	x	6	4	20	26	3	4	19	12
	Z	-2.8	-3.4	0.8	2.3	-1.2	-0.7	6.0	2.9
Feb. 95	N	120	120	120	120	36	36	36	36
	x	10	24	8	5	8	2	5	4
	Z	-1.4	2.5	-1.9	-2.8	1.8	-1.3	0.3	-0.2
April 95	N	153	153	153	153	55	55	55	55
	x	12	11	27	9	11	4	26	1
	Z	-1.7	-2.0	1.9	-2.5	1.7	-1.2	7.8	-2.4
June 95	N	91	91	91	91	36	36	36	36
	x	1	39	6	4	1	6	3	4
	Z	-3.3	8.8	-1.7	-2.3	-1.8	0.8	-0.8	-0.2

As mentioned previously, N is a total number of possible unidirectional pairs, x is observed number of pairs representing a particular case

in one of the two opposing directions, and Z is Z-statistics ($\frac{x-Np}{\sqrt{Npq}}$). In October, 1994, the 16 samples (n) provide a possible 128 (N) "seaward trending" pairs and, conversely, 128 "landward trending". Of possible cases indicative of a transport direction, either case B or case C is not significant during the October of 1994. However, when we only see the sand ridge area in Line-D, the 9 samples (n) contain a possible 36 (N) "seaward trending" pairs and, conversely, 36 "landward trending". Here, only case B (finer, bettered-sorted, and more negatively skewed) in the landward trending is significant with Z value of 7.3 (Table 1). During the period of December, 1994, the whole D-line does not show any transport direction but the sand ridge contains cases B and C in the landward trending. But, in the landward trending, case B (finer, better-sorted, and more negatively skewed) with Z value of 6.0 has higher significance than case C (coarser, better-sorted, more positively skewed) with Z value of 2.9 (Table 1). This indicates that both suspended sediments carrying fine grains and bedloads producing coarser grains exist together during the flood tide. In February, 1995, representing the mid-winter season, case C (coarser, better-sorted, and more positively skewed) with Z value of 2.5 is found in the whole Line-D, suggesting tidal energy increases seaward. On the other hand, case B in the seaward trend with Z value of 1.8 is recognized, indicating a decrease of ebb tidal energy within the sand ridge (Table 1). However, the seaward trending (either case C and case B) is not strongly significant in comparison with the period of Oct. and Dec. 1994. When the season is changed to early spring (April, 1995), case B in the landward trending with Z value of 1.9 in the whole Line-D is moderately significant, indicating a decrease of flood tidal energy. In the area of sand ridge, case B in both seaward ($Z = 1.7$) and landward trendings ($Z = 7.8$) are found, indicating that suspended sediments are prevalent in both ebb and flood currents, especially more significance of flood currents. Finally, in the beginning of summer season (June, 1995), case C of the seaward trend in the whole Line-D is found with a strong Z value of 8.8, suggesting strong energy regime seaward. In the sand ridge itself, no significant trend either seaward or landward is recognized, indicating no significant sediment transport (Table 1). The summery of Table 1 is simply presented in Table 2 with only the expression of cases B and C in the seaward and landward trend. When Z value is less than 1.65 (0.05 level of significance), the expression of "no" in Table 2, shows that no significant sediment transport occurred.

Table 2. The simplified list of the numbers of pairs of the whole and sand ridge itself of Line-D in Garolim Bay, presenting siginificant values of transport trends ($Z > 1.645$ with 0.05 level of significance) and the expression of "no" with no particular transport trends ($Z < 1.645$).

	Line-D (whole)				Line-D (Sand Ridge)			
Period	Seaward		Landward		Seaward		Landward	
	B	C	B	C	B	C	B	C
Nov. 94	no	no	no	no	no	no	7.3	no
Dec. 94	no	no	no	2.3	no	no	6.0	2.9
Feb. 95	no	2.5	no	no	1.8	no	no	no
April 95	no	no	1.9	no	1.7	no	7.8	no
June 95	no	8.8	no	no	no	no	no	no

7.2. Line-S

Line-S in the western part of middle Garolim Bay is expected to exhibit a much better transport trend because of similar grain-size distribution and monotonous geomorphic features (Figs. 1, 2, and 5). Five times of monitoring at the same period of the observation from Line-D were conducted. Interestingly, B case in either the seaward and landward trend is not found in Line-S (Table 3).

Table 3. The numbers of pairs of Line-S in Garolim Bay producing transport trends. N, x, and Z are defined in the text.

		Line-S			
Period		Seaward		Landward	
		B	C	B	C
Nov. 94	N	78	78	78	78
	x	1	41	3	12
	Z	-2.7	37.7	-2.1	0.7
Dec. 94	N	78	78	78	78
	x	0	48	10	6
	Z	-3.1	12.9	0.0	-1.2
Fed. 95	N	91	91	91	91
	x	0	48	11	19
	Z	-3.6	11.6	-0.1	2.4
April 95	N	91	91	91	91
	x	1	35	3	24
	Z	-3.2	7.5	-2.6	4.0
June 95	N	78	78	78	78
	x	0	22	5	22
	Z	-3.3	4.2	-1.6	4.2

The strong seaward trend by case C (coarser, better-sorted, and more positively skewed) is recognized in the whole monitoring period (from Oct. 1994 to June, 1995). This indicates that ebb tidal energy is stronger than flood tidal energy. Case C in the landward trend is found during February to June of 1995 with Z value of 2.4, 4.0, and 4.2, respectively. Also, the summary of Table 3 is presented in Table 4.

Table 4. The simplified list of the numbers of pairs of Line-S in Garolim Bay, with the same indication of Table 2.

	Line-S			
Period	Seaward		Landward	
	B	C	B	C
Nov. 94	no	37.7	no	no
Dec. 94	no	12.9	no	no
Fed. 95	no	11.6	no	2.4
April 95	no	7.5	no	4.0
June 95	no	4.2	no	4.2

8. Discussion and Conclusions

With the assumption of the sediment-transport path model proposed by *McLaren and Bowles* (1985), two locations, Line-D and Line-S in Garolim Bay were selected to test this model in the case of distinctive bidirectional transport area of tidal flats. Also, sequential monitoring from Oct. 1994 to June, 1995 is conducted for the comparison among time-series. The model shows that sediments become coarser in the direction of transport with an increasing energy regime in the Line-S area, indicating strong ebb-tides during the period of observation. It is noted that seasonal trends are also found in case C of the seaward trend in Line-S, showing a decreasing Z value, starting from Oct. 1994 to June, 1995 (Table 4). The highest energy regime in the seaward trend (case C with Z value of 37.7) occurred during the period of Oct. 1994 (the beginning of the winter season) in Line-S. The energy regime decreases slightly during Dec. and Feb. 1994 with Z value of 12.9 and 11.6, respectively. However, these values still indicate high energy regimes during these periods (the winter season) in Line-S. In the early spring, the energy regime started decreasing rapidly (Z = 7.5), but this energy is still significantly strong. Finally, during the beginning of the summer (June, 1995), another sharp decrease of energy regime (Z = 4.2) occurred in Line-S. The decreasing trend of energy regime of Line-S (case C of the seaward trend) shows that the seasonal changes of energy regime can be recognizable from this test. Even though, in Line-S, the energy regime is high enough to compare with case C of the seaward trend, case C of the landward trend shows a slight increasing trend of energy regime from Feb. to June, 1995 (Z value of 2.4, via 4.0, to 4.2), indicating flood tidal currents become stronger toward the summer season (Table 4).

Contrasted to Line-S, Line-D does not show a consistent and distinctive trend of sediment transport either seaward and landward (Tables 1 and 2) during the observed period. This is related to complex geomorphic features in the Line-D area (see Fig. 5 and the description of surface morphology in section 6.) As mentioned before, the whole area and sand ridge itself in Line-D area are separately tested by this model because sediment transport processes in muddy sand flat in the landside area are more affected by the adjacent tidal channel directly connected to the baymouth (Figs 1 and 2). Case B of the seaward trend is not found in the whole Line-D area (Table 2), but minor significance of the seaward trend for case B is shown in the sand ridge itself during Feb to April of 1995 with Z value of 1.8 and 1.7, respectively. The movement of finer sediment seaward occurred from the mid-winter season to the beginning of spring indicates that ebb tidal currents decrease seaward in this period. But this event only occurs during this season. On the other hand, two events (Feb. and June of 1995) of the coarsening trend landward (case C) are found in the whole Line-D (Tables 1 and 2), but no coarsening seaward trend (case C) is shown in the sand ridge. The distintive fining trend landward (case B) occurred in the sand ridge itself, showing Z value of 7.3 in Oct., 1994, of 6.0 in Dec., 1994, and of 7.8 in April, 1995. This scattered data do not represent seasonal changes, suggesting further investigation in the future needed. Case C of the landward trend in the whole Line-D is significant with Z value of 1.9 in April, 1995, but this value is controllled by the strong Z value of 7.8 calcuated from the sand ridge itself at that time (Tables 1 and 2). One event of case C of the landward trend is found in the sand ridge itself and the whole Line-D during the period of Dec., 1994. Also, the Z value of 2.3 in the whole Line-D is resulted from the Z value of 2.9 in the sand ridge itself, indicating that no sediment transport occurred in the muddy sand flat and its adjacent tidal channel in the landside area.

Even though more complicated situations ane involved in the study area compared to data from sedimentary environments containing unidirectional currents, the sediment-transport path model provides more clear quantitative trend of sediment transport for both ebb and flood currents on the tidal flats in the study area. Also, the first test of this model for sequential comparison among time-series shows that more expanded temporal and spacial areas can be applicable in many geological areas.

Acknowledgements

This research was funded from the grant of Korea Ocean Research and Development Institute (PE00544). Many thanks are extended to all friends in Marine Geology Group of KORDI, especially to H. J. Lee, H. J. Woo, H. D. Chang, J. H. Chun, S. Chang, S. J. Kwon, and K. S. Kim for their great assistance in the field and laboratory.

References

Day, T. J. A study of the transport of graded sediments : Report No. IT 190, Hydraulics Research Station, Wallingford, England, pp. 11, 1980.

Emmett, W. W., R. M. Myrick, and R. H. Meade, Field data describing the movement and stroage of sediment in the East Fork River, Wyoming. Part I. River hydraulics and sediment transport, 1979 : United States Department of the Interior, Geological Survey, Open File Report, 80-1189, pp. 43, 1980.

Folk, R. L. Petrology of Sedimentary Rocks. pp. 57, Hemphill, Austin Tex., 1974.

Griffith, J. C. Scientific method in analysis of sediments, pp. 508, McGraw-Hill, New

York, 1967.

Han, S.J., The clay mineralogy of recent sediment in Garolim Bay. Korea. Journal of Geological Society of Korea, 18, 215-220, 1982.

Korea Meteorological Administration, Annual Climatological Report, Seoul, Korea, pp. 89, 1989.

Korea Meteorological Administration, Annual Climatological Report, Seoul, Korea, pp. 72, 1981.

Korea Meteorological Administration, Annual Climatological Report, Seoul, Korea, pp. 242, 1991,

Korea Ocean Research, and Development Institute, Hydrographical, meteorological, geophysical, sedimentological, ecological surveys and tidal model surveys - Feasibility studies of Garolim tidal power plant, Report No. BSPI 00027, 1981.

Korea Ocean Research, and Development Institute, A report of feasibility survey of tidal power plant in Garolim Bay, pp. 511, 1993.

McLaren, P., W.B. Barrie, and J.M., Sempels, The coastal morphology and sedimentology of Cape Hatt : implications for the Baffin Island Oil Spill Project (BIOS), in Current Research, Pt. B, Geol. Surv. Canada, Pap. 81-1B, 153-162, 1981.

McLaren, P., The Whytecliff oil spill, British Columbia : sediment trends and oil movement on a beach, in Current Research, Pt. A, Geol Surv. Canada, Pap. 84-1A, 81-85, 1984.

McLaren, P., and D. Bowles, The effects of sediment transport on grain-size distributions, J Sed. Petro., 55, 0457-0470, 1985.

Pickrill, R.A., and J. Irwin, Sedimentation in a deep glacier-fed lake-Lake Tekapo,, New Zealand, sedimentology, 30, 63-75, 1983.

Shin, D.H., H.I. Yi, S.J. Han and J.K. Oh, Sedimentary Processes on the Tidal Flats of Garolim Bay, the Mid-western Coast of Korea, Abstract Volume of the Third International Conference on Asian Marine Geology : Evolution and Dynamics of the Asian Seas, Cheju, Korea, 1995a.

Shin, D.H., H.I. Yi, S.J. Han, and J.K. Oh, Changes in Sedimentary Processes and Environments on the Tidal Flats of Garolim Bay, the Western Coast of Korea, Abstract Volume of 2nd Annual Meeting of International Geological Correlation Program Project 367 : Late Quaternary Coastal Records of Rapid Change : Application to Present and Future Condition, Antofagasta, Chile, 1995b.

Shin, D.H., H.I. Yi, S.J. Han, and J.K. Oh, Relations of Sedimentary Processes to Depositional Environments on the Tidal Flats of Garolim Bay, the Western Coast of Korea, Quaternary Science Review, in press (1995c)

Song, W.O., D.H. Yoo and K.R. Dyer, Sediment Distribution, Circulation and Provenance in a Macrotidal Bay : Garolim Bay, Korea. Marine Geology, 52, 121-140, 1983.

Spiegel, M.R., Theory and Problems of Statistics : Schaum's Outline series, 359 pp., McGraw-Hill Book, New York, 1961.

Yi, H.I., D.H. Shin, S.J. Han, and J.K. Oh, Seaonal Changes in Sedimentary Environments of Garolim Bay, the Western Coast of Korea, Abstract Volume of 1995 Fall Meeting of the Korea Quaternary Association, Seoul, Korea, 1995.

Yi, H.I., D.H. Shin, S.J. Han, and J.K. Oh, Modern Sedimentary Environments in Comparison with Sedimentary Sequences in Garolim Boy of the Korean Coast, Abstract volume of the 30th International Geological Congress, Beijing, China, in press (1996).